# Preparation and Characterization of Microporous Polyethylene Hollow Fiber Membranes

**LI-QIANG SHEN, ZHI-KANG XU, YOU-YI XU**

Institute of Polymer Science, Zhejiang University, Hangzhou 310027, China

*Received 25 October 2000; accepted 26 July 2001*

**ABSTRACT:** Microporous polyethylene (PE) hollow fiber membrane with a porosity of 43% and $N_2$ permeation of 4.96 $cm^3$ (STP)/$cm^2$ s cmHg was prepared by melt-spinning and cold-stretching method. It was found that PE with a density higher than 0.96 g/$cm^3$ should be used for the preparation of microporous PE hollow fiber membranes. By increasing the spin–draw ratio, both the porosity and the $N_2$ permeation of the hollow fiber membranes increased. Annealing the nascent hollow fiber at 115°C for 2 h was suitable for attaining membranes with good performance. By straining the hollow fiber to higher extensions, the amount and size of the micropores in the hollow fiber wall increased, and the $N_2$ permeation of the membranes increased accordingly. © 2002 John Wiley & Sons, Inc. J Appl Polym Sci 84: 203–210, 2002; DOI 10.1002/app.10305

**Key words:** polyethylene; membrane; morphology

## INTRODUCTION

Microporous membranes fabricated from hydrophobic polymers such as polyethylene (PE) and polypropylene (PP) have great advantages over hydrophilic membranes made from polyacrylonitrile, cellulose, and others when used in fields such as membrane distillation and membrane extraction because of their strong hydrophobicity.[1] Generally speaking, there are two ways to prepare polyolefin membranes: thermally induced phase separation (TIPS)[2,3] and melt-spinning and cold-stretching (MSCS).[4–7]

For the TIPS method, the polymer and diluent are mixed to form homogenous solution at elevated temperatures. Upon cooling, the system undergoes liquid–liquid or solid–liquid phase separation, which results in the formation of polymer-rich and diluent-rich phases. After solidification of the polymer-rich phase, the diluent is extracted and the sites occupied by the diluent are left to form the microporous membrane. Therefore, by selecting appropriate diluents and cooling conditions, is relatively convenient to the control the pore size. However, it is obvious that this process results in a waste solvent problem. On the other hand, the MSCS method does not need any solvent, which is more environment-beneficial than the TIPS method. The micropores of the membranes in the MSCS process are formed by stretching the pure polymer hollow fiber or film. This means that the MSCS process does not involve any phase separation and its handling is relatively easy.

As we know, the preparation of microporous polyolefin hollow fiber membranes through MSCS method is based on the hard elastic property of the materials. That is, under proper conditions, the melt-spinning hollow fibers fabricated from highly crystalline polymers such as PE and PP may exhibit high-elastic recovery such as elas-

*Correspondence to:* Z.-K. Xu (xuzk@ipsm.zju.edu.cn).

Contract grant sponsor: National Natural Science Foundation of China; contract grant number: 59673030.

Journal of Applied Polymer Science, Vol. 84, 203–210 (2002)

tomers and high-yield stress such as normal plastics.[8] The lamellae in hard elastic fibers aligned in rows normal to the fiber direction. Upon straining, they will separate and micropores bridged by fibrils will be formed. Then, if the fibers are heat-set, macromolecular chains in the fibrils will reorder or recrystallize to form stable structure and the micropores are fixed. During the formation of the micropores, there are many factors which would influence the micropore structure, for example, the spinneret temperature, the melt-draw ratio, and the annealing condition.[4]

There has been much literature, mainly patents, that described the preparation of microporous PP or PE hollow fiber membranes through the MSCS method.[4–6] However, there were few detailed investigations about the factors that influence the membrane structures.[7] In this article, factors such as spin–draw ratio, annealing temperature and time, and fiber extension on the preparation of microporous PE hollow fiber membranes were discussed.

## EXPERIMENTAL

### Materials

Two types of high-density PEs were used. Yangtze 5000S with a melt index of 1.08 g/10 min was purchased from Yangtze Petrochemical Co. (China) and Hi-Zex 2200J with a melt index of 5.4 g/10 min was purchased from Mitsui Petrochemical Co., Ltd. (Japan). High-purity nitrogen (99.99%) was used for the gas permeation measurement of the membranes.

### Preparation of Microporous PE Hollow Fiber Membranes

The melt-spinning system was the same as was used in Hangzhou Hualu Membrane Engineering Co., Ltd. A tube-in orifice spinneret with inner and outer diameters of 9 and 13 mm was used. First, the PE melts were extruded out of the spinneret at 190°C by using nitrogen as bore gas. Then, the hollow fibers were taken up at a spin–draw ratio of 680 and annealed for 2 h at 115°C. Subsequently, the hollow fibers were strained to low extensions at temperatures lower than 40°C and then to 130% at temperatures higher than 80°C. At last, the hollow fibers were heat-set at 110°C for 30 min. All the preparation parameters are same as described above unless specified otherwise.

### Characterization

#### *Crystallinity*

A Perkin–Elmer DSC 7 was used to measure the crystallinity ($X_c$) of the sample at a heating rate of 10°C/min. The crystallinity was defined as

$$X_c\ (\%) = \Delta H/\Delta H^0 \times 100$$

where $\Delta H$ is the measured heat of fusion for the sample, and $\Delta H^0$ is the theoretical heat of fusion for the pure PE crystal (taken as 293 J/g).[9]

#### *Morphologies of the Samples*

The morphologies of the samples were examined by using a Hitachi S-570 scanning electron microscopy (SEM) at an accelerating voltage of 20 kV. The surfaces of the samples were coated with a thin film of gold to prevent charging prior to the SEM examinations.

#### *Mechanical Property*

The elastic recoveries of the hollow fibers were tested by using an XL-250A tensile testing machine (Guangzhou Test Instrument Factory). The elastic recovery ($E_r$) was defined as

$$E_r\ (\%) = (l_1 - l_2)/(l_1 - l_0) \times 100$$

where $l_0$ is the fiber length before straining, $l_1$ is the fiber length when strained to 100%, and $l_2$ is the fiber length when the load was returned to zero after strained to 100%.

#### *Porosity*

The porosity ($P$) of the hollow fiber membrane was determined with a density method. A certain length of hollow fiber was weighed. The outer and inner diameters of the hollow fiber were measured as an average of 10 samples by using a microscope. Then the density ($\rho$) of the hollow fiber was defined as

$$\rho = \frac{W}{\pi(R^2 - r^2)l}$$

**Table I Hollow Fibers Spun from Different PEs**

| Type of PE | Melt Index (g/10 min) | Density ($g/cm^3$) | Crystallinity (%) | $E_r$ of Hollow Fiber before Straining (%) | Porosity (%) | $N_2$ Permeation[a] |
|---|---|---|---|---|---|---|
| Hi-Zex 2200 J | 5.40 | 0.968 | 93.1 | 82 | 34 | $4.35 \times 10^{-2}$ |
| Yangtze 5000 S | 1.08 | 0.955 | 82.8 | 45 | 0 | 0 |

[a] Unit of $N_2$ permeation is $cm^3$ (STP)/$cm^2$ s cmHg.

where $W$ is the weight of the hollow fiber, $R$ and $r$ are the outer and inner diameters, respectively, and $l$ is the length of the hollow fiber.

Thus, the porosity of the hollow fiber membrane was defined as

$$P\ (\%) = (\rho_0 - \rho_1)/\rho_0 \times 100$$

where $\rho_0$ is the density of the hollow fiber before straining and $\rho_1$ is the density of the hollow fiber after straining.

### *$N_2$ Permeation*

About 10 hollow fiber membranes were bundled in a U-shape and their open ends were fastened with epoxy resin to fabricate a module. The length of every hollow fiber membrane was about 10 cm. Then, a nitrogen pressure of 15 cmHg was applied to the inside of the hollow fiber membrane at 25°C, and the amount of nitrogen that permeated through the membrane was determined. The $N_2$ permeation ($F$) was calculated according to the following equation

$$F = \frac{V_{N_2}}{A \times P \times t}$$

where $V_{N2}$ is the nitrogen volume that permeates through the membrane, $A$ is the membrane area that is calculated on the basis of the inner diameter of the hollow fiber membrane, $P$ is the nitrogen pressure between the upside and downside of the membrane, and $t$ is the time when nitrogen permeates through the membrane.

## RESULTS AND DISCUSSION

### Hollow Fibers Spun from Different Types of PEs

It was reported that PEs with density higher than 0.96 $g/cm^3$ should be used to gain PE hollow fibers with good hard elasticity.[10–12] Because hard elasticity is the basis of microporosity of PE hollow fiber membranes, it is important to select proper PE materials for the spinning of microporous PE hollow fiber membranes. In this study, two types of PEs, Yangtze 5000S and Hi-Zex 2200J, were used.

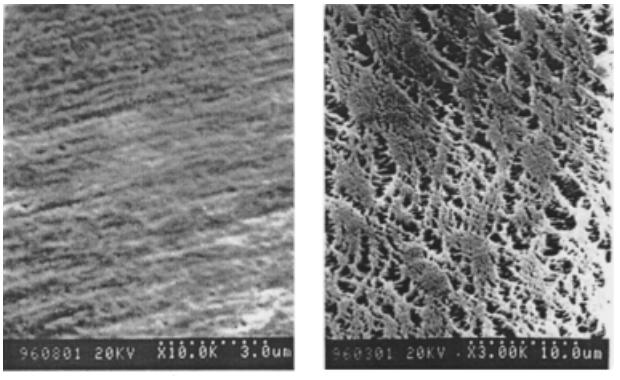


**Figure 1** SEM micrographs of the outer surfaces of strained hollow fibers spun from (a) Yangtze 5000S (a) and (b) Hi-Zex 2200J. Magnification: ×10,000 (a) and ×3000 (b).

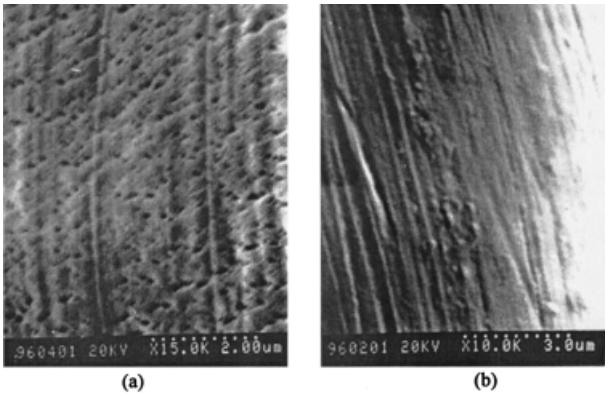


**Figure 2** SEM micrographs of the outer surfaces of annealed hollow fibers spun from (a) Hi-Zex 2200J and (b) Yangtze 5000S. Magnification: ×15,000 (a) and ×10,000 (b).

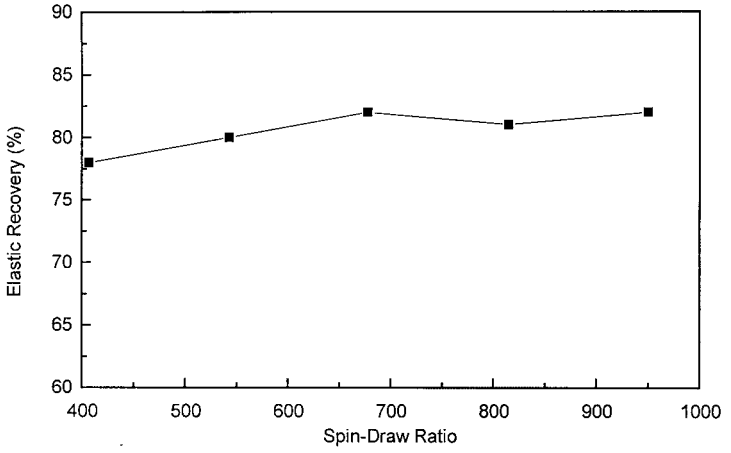


**Figure 3** Relationship between spin–draw ratio and elastic recovery of unstrained hollow fiber.

As shown in Table I, before straining, the resulting hollow fibers exhibit very different elastic recovery, which indicates different hard elasticity. It is well known that higher elastic recovery means better hard elasticity. Data shown in Table I reveal that the hollow fiber spun from Hi-Zex 2200J exhibits higher elastic recovery just like other kinds of hard elastic fibers; however, the hollow fiber spun from Yangtze 5000S performs more like normal PE fibers. After these two kinds of hollow fibers were strained to the same extension of 130% and heat-set, the hollow fiber spun from Yangtze 5000S shows a $N_2$ permeation of 0 and a porosity of 0, whereas the hollow fiber spun from Hi-Zex 2200J exhibits just the opposite properties. The results were confirmed by the SEM micrographs of the hollow fibers. In Figure 1(a) for Yangtze 5000S, no micropore can be seen in the fiber wall, whereas there are many interconnected micropores in Figure 1(b) for Hi-Zex 2200J.

The reason for this result may be complicated because there are many factors that influence the preparation of microporous PE hollow fiber membranes. It was pointed out that two important factors which are in favor of hard elasticity are perfect crystal structure and amorphous region with good mobility.[13] It can be seen from Table I that Hi-Zex 2200J shows higher crystallinity and higher density. Thus, it may be easier for Hi-Zex 2200J to form relatively perfect crystal structure when extruded from spinneret than Yangtze 5000S. Moreover, the higher melt index of Hi-Zex 2200J, which indicates lower molecular weight,

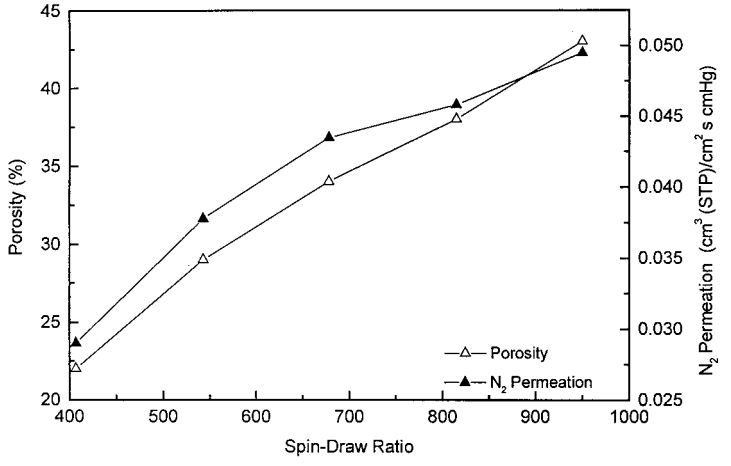


**Figure 4** Relationship between spin–draw ratio and properties of hollow fiber membrane.

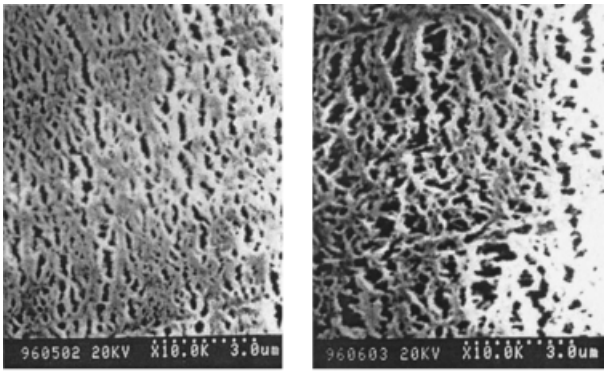


**Figure 5** SEM micrographs of the outer surfaces of hollow fiber membranes spun with spin–draw ratio of (a) 680 and (b) 950. Magnification: ×10,000.

may contribute to the higher mobility of the amorphous regions, which is in favor of the formation and closing of microvoids under extension. Therefore, with more perfect crystal structures and more mobile amorphous regions, the hollow fibers spun from Hi-Zex 2200J exhibit better hard elasticity than the hollow fibers spun from Yangtze 5000S. This is consistent with the literature.[10–12] Consequently, after straining and heat-setting, the hollow fibers spun from Hi-Zex 2200J show micropores in its wall, whereas hollow fibers spun from Yangtze 5000S do not, as illustrated in Figure 1(a,b).

Figure 2(a) shows that the hollow fiber spun from Hi-Zex 2200J possesses well-formed thick crystalline lamellae perpendicular to the fiber direction, which is a main feature of hard elastic fiber. However, it can be seen from Figure 2(b) that the wall of the hollow fiber spun from Yangtze 5000S is similar to that of ordinary oriented hollow fiber. These fibers indicate that the hollow fiber from Hi-Zex 2200J has good hard elasticity, whereas that from Yangtze 5000S does not.

As a result of the above discussion, Hi-Zex 2200J was used only in the following investigation.

### Effect of Spin–Draw Ratio

The effect of spin–draw ratio on the resulting hollow fiber properties was examined and the results are illustrated in Figures 3 and 4. Figure 3 shows that the elastic recoveries of the unstrained hollow fibers increased slightly with increasing spin–draw ratios. In addition, the porosities and $N_2$ permeations of the microporous hollow fiber membranes both increase with increasing spin–draw ratios, as illustrated in Figure 4.

One possible explanation for the phenomena may be that the higher spin–draw ratio can stimulate the formation of more perfect row-nucleated crystals, which increases hard elasticity of the unstrained hollow fibers. Besides, more perfect oriented crystalline lamellae can contribute to the formation of more and larger micropores in the fiber wall, which increases the membrane porosity and gas permeation. Figure 5(a,b) illustrates the morphologies of the resulting hollow fibers spun from spin–draw ratios of 680 and 950. The SEM micrographs show clearly that the micropores of the hollow fiber spun with spin–draw ratio of 950 are more and larger than those of the hollow fiber spun with spin–draw ratio of 680.

### Effect of Annealing

After the hollow fiber is spun from the spinneret and taken up, it should be annealed below the melting point of PE to increase elasticity of the hollow fiber; then the micropores can be more readily formed in the fiber wall during the strain-

**Table II Hollow Fibers Annealed at Different Temperatures**

| Annealing Temperature (°C) | Hollow Fiber before Straining | | Hollow Fiber after Straining | |
|---|---|---|---|---|
| | $E_r$ (%) | Crystallinity (%) | $N_2$ Permeation[a] | Porosity (%) |
| No annealing | 51 | 86 | — | — |
| 90 | 70 | 88 | $3.70 \times 10^{-2}$ | 29 |
| 110 | 74 | 89 | $4.08 \times 10^{-2}$ | 32 |
| 115 | 82 | 90 | $4.35 \times 10^{-2}$ | 34 |

[a] Unit of $N_2$ permeation is $cm^3$ (STP)/$cm^2$ s cmHg.

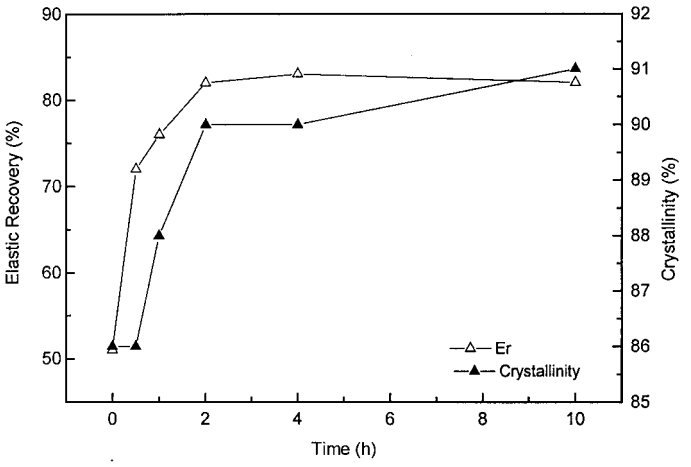


**Figure 6** Relationship between annealing time and properties of annealed hollow fiber.

ing process. In the annealing process, annealing temperature and time are the two key factors influencing structure and properties of the hollow fiber membranes.

After the hollow fibers are extruded out of the spinneret, they rapidly undergo stress crystallization and hence the row-nucleated crystals form. However, the process is so short that there are many molecular chains that align irregularly in lamellae; thus, many defects exist after the hollow fibers are taken up. Upon annealing under proper conditions, these unstable defects will reorder to form more perfect structures. The result is that the defects will reduce and more stable crystals will form. Moreover, density of the hollow fiber will show some increase because of higher crystallinity, as has been mentioned by Kim et al.[7] Thus, the elasticity of the hollow fiber improves after annealing. This phenomenon was observed in this study also. As shown in Table II, the elastic recoveries of the annealed hollow fibers enhance to a great extent in contrast to the unannealed hollow fiber. Besides, it can be seen that the elastic recoveries of the unstrained hollow fibers increased with increasing annealing temperatures in Table II. This may be that higher annealing temperature is in favor of the rearranging of imperfect regions in the fiber wall. As a result of improved elasticity, the micropores in the fiber wall formed more easily when the hollow fiber was strained; the porosity and $N_2$ permeation of the hollow fiber membrane both increased. Within the temperature scope examined in this study, hollow fiber membrane with higher

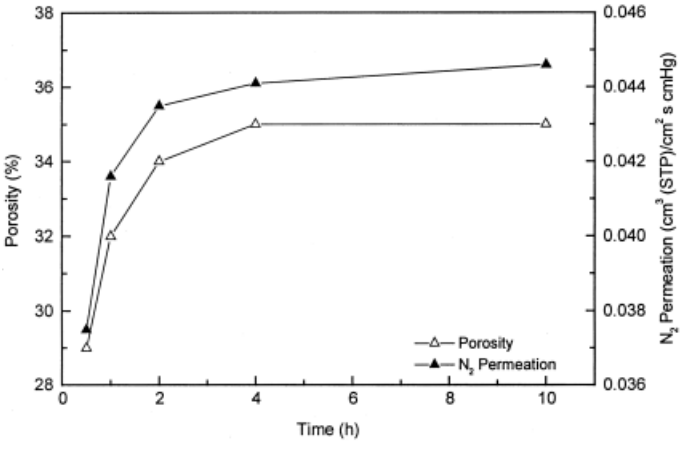


**Figure 7** Relationship between annealing time and properties of strained hollow fiber.

**Table III Microporous Hollow Fibers Strained to Different Extensions**

| Extension (%) | $N_2$ Permeation[a] | Porosity (%) | OD/ID ($\mu$m/$\mu$m) |
|---|---|---|---|
| 100 | $3.78 \times 10^{-2}$ | 30 | 415/375 |
| 130 | $4.35 \times 10^{-2}$ | 34 | 409/369 |
| 170 | $4.96 \times 10^{-2}$ | 43 | 394/357 |

[a] Unit of $N_2$ permeation is $cm^3$ (STP)/$cm^2$ s cmHg.
OD, outer diameter of hollow fiber; ID, inner diameter of hollow fiber.

porosity and $N_2$ permeation can be obtained at higher annealing temperatures.

In addition, the effect of annealing time was examined in this study. Figure 6 shows that the elastic recovery and crystallinity of the hollow fiber increase with increasing annealing time in the initial stage of about 2 h. However, more annealing time has almost no influence on the elastic recovery and crystallinity of the hollow fiber. The explanation may be that the reordering of the molecular chains in the fiber wall is a dynamic process, which needs some time to fulfill. Once the process is mostly completed, increasing the annealing time further has no effect. Thus, the properties of the hollow fiber did not change much after about 2 h of annealing. Because of the changes of the hollow fiber in elasticity and crystallinity, the porosity and $N_2$ permeation of the strained hollow fiber change accordingly. As shown in Figure 7, similar to the curves shown in Figure 6, the curves level off also above annealing time of 2 h. All these results indicate that about 2 h of annealing is proper for obtaining hollow fibers with reasonable performances in this study.

### Effect of Extension

The micropores of PE hollow fibers are formed by straining. For a typical process of straining, the hollow fibers were first strained to lower extensions under somewhat low temperatures to induce microvoids in the fiber wall. Then, the hollow fibers were strained to higher extensions under higher temperatures to form more and larger micropores without the breaking of the hollow fibers.

In this study, the PE hollow fibers were strained to different extensions and heat-set at 110°C for 30 min. The results are presented in Table III. As can be seen, the porosity and $N_2$ permeation of the hollow fibers increased with increasing extensions. Figure 8 shows the SEM micrographs of the hollow fibers with different extensions. It is obvious that the amount and size of the micropores increased with increasing extensions.

When a hard elastic fiber is strained,[14] first, the lamellae of the fiber rotate, that is, the *c*-axis of the lamellae originally perpendicular to the fiber direction rotates to a position parallel to the fiber direction. Then, the lamellae are separated and the molecular chains of amorphous regions are oriented; thus, the microvoids bridged by fibrils are created. If the fiber is extended further, molecular chains in the lamellae will be pulled out at higher extensions, and larger and more microvoids can be formed, but the cross-sectional area of the fiber will reduce markedly. The result of increased porosity and gas permeation with increasing extensions in this study confirms the abovementioned theory. Moreover, in this study, the inner and outer diameters of the unstrained hollow fiber are 395 and 440 $\mu$m, respectively. In comparison with the data listed in Table III, it

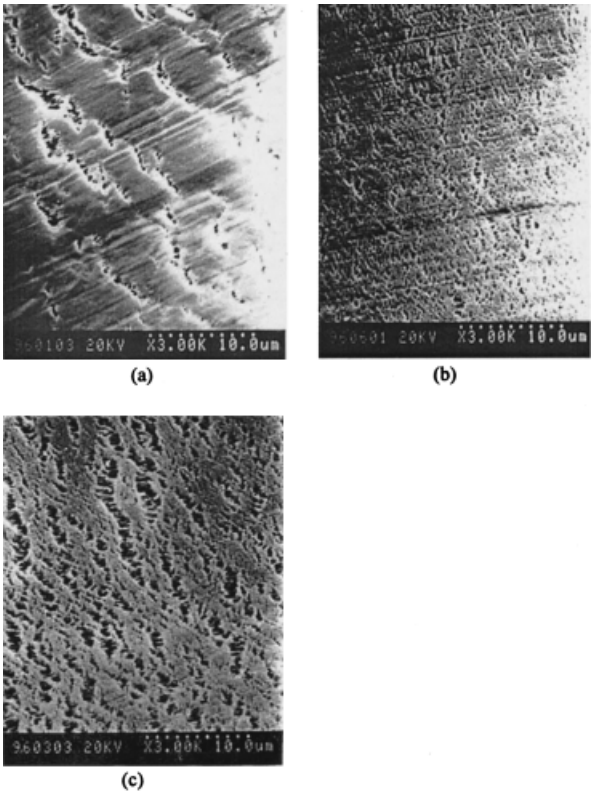


**Figure 8** SEM micrographs of the outer surface of hollow fiber membranes with different extensions: (a) extension of 100%, (b) extension of 130%, and (c) extension of 170%. Magnification: ×3000.

can be concluded that the cross-sectional areas of the fibers reduce a great deal, which is another proof for the theory.

The financial support of the National Natural Science Foundation of China (Grant No. 59673030) is gratefully acknowledged.

## REFERENCES

1. Couffin, N.; Cabassud, C.; Lahoussine-Turcaud, V. Desalination 1998, 117, 233.
2. Matsuyama, H.; Berghmans, S.; Lloyd, D. R. Polymer 1999, 40, 2289.
3. Atkinson, P. M.; Lloyd, D. R. J Membr Sci 2000, 175, 225.
4. Jun, K.; Takayuki, H.; Hiroshi, T.; Kenji, K. Eur Pat. Appl. 0498,414, A2, 1992.
5. Nagano, H.; Matsunami, K.; Yashida, K. Jpn Kokai Tokyo 52,137,026, 1977.
6. Mitsubishi Rayon Co. Jpn Kokai Tokyo 57,42,919, 1982.
7. Kim, J. J.; Jang, T. S.; Kwon, Y. D.; Kim, U. Y.; Kim, S. S. J Membr Sci 1994, 93, 209.
8. Cannon, S. L.; McKenna, G. B.; Statton, W. O. J Polym Sci, Macromol Rev 1976, 11, 209.
9. Runt, J. P. in Encyclopedia of Polymer Science and Engineering, 2nd ed.; Kroschwitz, J. I., Ed.; John Wiley and Sons: New York, 1986; Vol. 4, p 487.
10. Kamei, E. Jpn Kokai Tokyo 63,35,818, 1988.
11. Shindo, M.; Yamamoto, T.; Fukunaga, O.; Yamamori, H. Jpn Kokai Tokyo 63,35,726, 1988.
12. Koshoji, T.; Shimizu, Y.; Yamazaki, T. Jpn Kokai Tokyo 02,112,404, 1990.
13. Du, Q. G.; Lin, M. D.; Yu, T. Y. J Fudan Univ (Nat Sci) 1986, 25, 375.
14. Samuels, R. J. J Polym Sci, Polym Phys Ed 1979, 17,535.